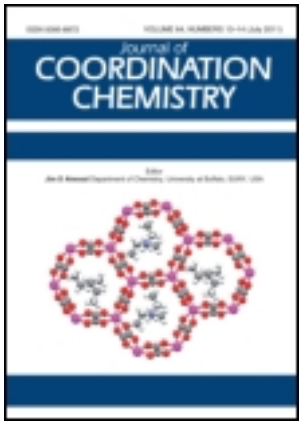


Journal of Coordination Chemistry
Publication details, including instructions for authors and subscription information:
http://www.tandfonline.com/loi/gcoo20

# Synthesis, spectroscopy, thermal behavior, and X-ray crystal structure of two lead(II) complexes with 4′-(4-tolyl)-2,2′;6′,2″-terpyridine (ttpy)

Lotfali Saghatforoush [a], Karim Adil [b], Ertan Şahin [c], Somayyeh Babaei [a] & Seyid Javad Musevi [d]

[a] Chemistry Department, Payame Noor University, Tehran 19395-4697, Islamic Republic of Iran

[b] Laboratoire des Oxydes et Fluorures, Universite du Maine, CNRS UMR 72085, Le Mans Cedex 9, France

[c] Department of Chemistry, Atatürk University, 25240 Erzurum, Turkey

[d] Department of Chemistry, Shahid Beheshti Technical Faculty, Technical and Vocational University, Urmia, Islamic Republic of Iran

Published online: 02 Dec 2011.

To cite this article: Lotfali Saghatforoush, Karim Adil, Ertan Şahin, Somayyeh Babaei & Seyid Javad Musevi (2011) Synthesis, spectroscopy, thermal behavior, and X-ray crystal structure of two lead(II) complexes with 4′-(4-tolyl)-2,2′;6′,2″-terpyridine (ttpy), Journal of Coordination Chemistry, 64:24, 4421-4433, DOI: 10.1080/00958972.2011.640395

To link to this article: http://dx.doi.org/10.1080/00958972.2011.640395

*Journal of Coordination Chemistry*
Vol. 64, No. 24, 20 December 2011, 4421–4433





# Synthesis, spectroscopy, thermal behavior, and X-ray crystal structure of two lead(II) complexes with 4′-(4-tolyl)-2,2′;6′,2″-terpyridine (ttpy)

LOTFALI SAGHATFOROUSH*†, KARIM ADIL‡, ERTAN ŞAHIN§, SOMAYYEH BABAEI† and SEYID JAVAD MUSEVI¶

†Chemistry Department, Payame Noor University, Tehran 19395-4697, Islamic Republic of Iran
‡Laboratoire des Oxydes et Fluorures, Universite du Maine, CNRS UMR 72085, Le Mans Cedex 9, France
§Department of Chemistry, Atatürk University, 25240 Erzurum, Turkey
¶Department of Chemistry, Shahid Beheshti Technical Faculty, Technical and Vocational University, Urmia, Islamic Republic of Iran

(*Received 1 September 2011; in final form 20 October 2011*)

Two new lead(II) complexes with 4′-(4-tolyl)-2,2′;6′,2″-terpyridine (ttpy), $[Pb(ttpy)(\mu\text{-}AcO)]_2(PF_6)_2$ (**1**) and $[Pb(ttpy)(\mu\text{-}AcO)I]_2$ (**2**), have been synthesized and characterized by CHN elemental analysis, $^1H$ NMR, $^{13}C$ NMR, IR spectroscopy, and structurally analyzed by X-ray single-crystal diffraction. The thermal stability of these compounds has been studied by thermal gravimetric analysis and differential thermal analysis. Single crystal X-ray analysis shows that **1** and **2** are dimeric units with Pb–$(\mu\text{-}AcO)_2$–Pb-type bridging, and the coordination number in **1** is six and in **2** is seven. The arrangement of donors suggests a gap in the coordination geometry around lead, possibly occupied by stereo-active lone pair of electrons on lead(II), so the coordination sphere is hemidirected. Furthermore, dimeric units are connected by a network of hydrogen bonds and $\pi$–$\pi$ stacking as well. Electrochemical properties of free ligand and complexes have been investigated in the presence of tetrabutyl ammonium perchlorate as supporting electrolyte and by using a glassy carbon electrode. Both lead complexes show irreversible Pb(II) oxidation. Cyclic voltammetry indicates that these processes are diffusion-controlled. The data from electrochemical studies show that the total limiting current of each of the studied complexes corresponds to two-electron transfer.

*Keywords*: 4′-(4-Tolyl)-2,2′; 6′,2″-terpyridine; Lead complexes; Crystal structure; Electrochemical studies

## 1. Introduction

Crystal engineering and metal ion chemistry of pyridine-based ligands have been extensively studied [1, 2]. Due to the ability of terpyridines to coordinate to a wide variety of metal ions by different coordination, they lead to complexes with special electronic and structural properties [3–5]. In particular, 2,2′;6′,2″-terpyridine and its

*Corresponding author. Email: saghatforoush@gmail.com


ISSN 0095-8972 print/ISSN 1029-0389 online © 2011 Taylor & Francis
http://dx.doi.org/10.1080/00958972.2011.640395

derivatives have attracted much interest [6, 7]. 4′-Tolyl-2,2′;6′,2″-terpyridine (ttpy) was first reported by Calzaferri in 1985 and improved syntheses have since been described [8–11].

In spite of interesting properties, main-group metal complexes have received less attention than transition metal coordination chemistry [12]. Among the main group elements, lead(II) complexes with N and O donors have been investigated due to the flexibility of lead and the coordination and stereoactivity of valence shell lone electron pair [13–23]. Lead may coordinate as holodirected, in which bonds to ligands are directed throughout the surface of an encompassing sphere, or may coordinate as hemidirected, in which bonds to ligands are directed throughout only part of a coordination sphere, leaving a gap in the distribution of bonds to the ligands. Pb(II) complexes with coordination numbers of two, three, four, and five are hemidirected while coordination numbers nine and ten are holodirected and coordination numbers six, seven and eight are often hemidirected [24]. Since it is not possible to directly detect the presence of a lone electron pair, it is common to relate the spatial distribution of surrounding donors to the presence and activity of a lone electron pair. An interesting point is that crystal packing may affect the size and extent of the lone pair in the coordination sphere [25].



## 2. Experimental

### 2.1. *Material and measurements*

All reagents were used as supplied by Merck and Aldrich without purification. $^{1}$H and $^{13}$C NMR spectra were measured with a BRUKER 400 UltraShield spectrometer at 400 MHz and all chemical shifts are reported in $\delta$ units downfield from $Me_4Si$. FT-IR spectra were recorded using a Thermo-Nicolet Nexus 670 spectrophotometer. Elemental analyses were carried out using a Heraeus CHN–Rapid analyzer. Melting points were measured on an Electrothermal 9100 apparatus. Thermal behavior was measured with a Mettler-Toledo TGA 851-E apparatus. Electrochemical experiments were carried out using an Autolab PGSTAT 20. Cyclic voltammograms of $10^{-3}$ mol L$^{-1}$ solutions in acetonitrile were recorded in an electrochemical cell, equipped with a Pt,Ag/AgCl and glassy carbon (GC) as counter, reference, and working electrode, respectively. Tetrabutylammonium perchlorate (TBAP) was used as supporting electrolyte and its concentration was $10^{-1}$ mol L$^{-1}$. The ferrocene–ferrocenium couple was used as an internal standard and $\Delta E_p$ of the $Fe/Fe^{+}$ couple under this experimental condition was 89 mV.

### 2.2. *X-ray crystallography*

For the crystal structure determination, single-crystals of the complexes were used for data collection on a four-circle Rigaku R-AXIS RAPID-S diffractometer (equipped with a 2-D area IP detector) and Bruker Kappa Apex II diffractometer. Graphite-monochromated Mo-K$\alpha$ radiation ($\lambda = 0.71073$ Å) and oscillation scans technique with $\Delta\omega = 5^{\circ}$ for one image were used for data collection. The lattice parameters were determined by least-squares on the basis of all reflections with

Table 1. Crystallographic data of **1** and **2**.

| Identification code | [Pb(ttpy)(μ-AcO)]$_2$(PF$_6$)$_2$ (**1**) | [Pb(ttpy)(μ-AcO)I]$_2$ (**2**) |
|---|---|---|
| Empirical formula | $C_{24}H_{20}F_6N_3O_2PPb$ | $C_{24}H_{20}IN_3O_2Pb$ |
| Formula weight | 734.59 | 716.52 |
| Temperature (K) | 293(2) | 293(2) |
| Wavelength (Å) | 0.71073 | 0.71073 |
| Crystal system | Triclinic | Triclinic |
| Space group | $P\bar{1}$ | $P\bar{1}$ |
| Unit cell dimensions (Å, °) | | |
| $a$ | 8.2818(6) | 8.674(5) |
| $b$ | 11.1780(9) | 9.552(5) |
| $c$ | 14.4511(11) | 14.297(5) |
| $\alpha$ | 75.926(4) | 79.701(5) |
| $\beta$ | 78.679(4) | 82.447(5) |
| $\gamma$ | 80.740(4) | 75.024(5) |
| Volume (Å$^3$), $Z$, $Z'$ | 1263.35(17), 2, 0 | 1121.4(10), 2,0 |
| Calculated density (g cm$^{-3}$) | 1.931 | 2.122 |
| Absorption coefficient (mm$^{-1}$) | 6.812 | 8.925 |
| $F$(000) | 704 | 672 |
| $\theta$ range for data collection (°) | 1.4–32.26 | 2.23–26.42 |
| Index ranges | $-12 \le h \le 12$;<br>$-16 \le k \le 16$;<br>$-21 \le l \le 21$ | $-9 \le h \le 10$;<br>$-11 \le k \le 11$;<br>$-17 \le l \le 17$ |
| Reflections collected | 8896 | 4564 |
| Independent reflections | 6593 | 4100 |
| Absorption correction | Empirical | Empirical |
| Refinement method | Full-matrix least-squares on $F^2$ | Full-matrix least-squares on $F^2$ |
| Data/restraints/parameters | 6953/0/330 | 4564/0/281 |
| Goodness-of-fit on $F^2$ | 0.968 | 1.075 |
| Final $R$ indices [$I > 2\sigma(I)$] | $R_1 = 0.0290$, $wR_2 = 0.0774$ | $R_1 = 0.0397$, $wR_2 = 0.0996$ |
| $R$ indices (all data) | $R_1 = 0.0483$, $wR_2 = 0.0970$ | $R_1 = 0.0458$, $wR_2 = 0.1083$ |
| Largest difference peak and hole (e Å$^{-3}$) | 1.055 and –1.138 | 1.454 and –1.355 |



$F^2 > 2\sigma(F^2)$. Integration of the intensities, correction for Lorentz and polarization effects, and cell refinement were performed using CrystalClear (Rigaku/MSC Inc., 2005) software. The structures were solved by direct methods using SHELXS-97 and refined by full-matrix least-squares using SHELXL-97. Hydrogen atoms were positioned geometrically and refined using a riding model. The final difference Fourier maps showed no peaks of chemical significance. The materials for publication were prepared using Mercury, Diamond, and ORTEP-3 programs [26]. Crystallographic data and details of the data collection and structure refinements are listed in table 1.

### 2.3. *Synthesis*

**2.3.1. Preparation of [Pb(ttpy)(μ-AcO)]$_2$(PF$_6$)$_2$ (1).** [Pb(ttpy)(μ-AcO)]$_2$(PF$_6$)$_2$ was prepared by a branched tube method: ttpy (1 mmol, 0.323 g) and ammonium hexafluorophosphate (2 mmol, 0.326 g) were placed in one arm of a branched tube and lead(II) acetate (1 mmol, 0.360 g) in the other. Methanol was carefully added to fill both arms, then the tube was sealed and the ligand-containing arm was immersed in

a bath at 60°C while the other was at ambient temperature. After two weeks, brown crystals were deposited in the cooler arm which were filtered off, washed with acetone, and air-dried (0.293 g, yield 50%), m.p. 287°C. Anal. Calcd for $C_{24}H_{20}N_3O_2PF_6Pb$ (%): C, 39.24; H, 2.75; N, 5.72. Found (%): C, 39.37; H, 2.92; N, 5.89. IR (KBr) ($\nu_{max}$, $cm^{-1}$): 3018 (C–H, arom); 2854 (C–H, aliph); 1421–1603 (C=C, arom); 1395 [$\nu_{sym}$(COO)] and 1571 [$\nu_{as}$(COO)]; 839 ($PF_6$). $^1$H NMR (DMSO) $\delta_H$: 1.69(3H, s, $CH_3$); 2.41(3H, s, $CH_3$); 7.42(2H, d, $^3J_{H-H} = 7.84$ Hz, arom); 7.61(2H, t, $^3J_{H-H} = 6.08$, 6.04 Hz, arom); 7.92(2H, d, $^3J_{H-H} = 7.76$ Hz, arom); 8.10(2H, t, $^3J_{H-H} = 7.75$, 7.69 Hz, arom); 8.73(2H, d, $^3J_{H-H} = 8.02$ Hz, arom); 8.76(2H, s, arom); 8.84(2H, d, $^3J_{H-H} = 4.36$ Hz, arom). $^{13}$C NMR (DMSO) $\delta_C$: 26.80, 117.65, 120.96, 124.57, 126.07, 130.05, 134.55, 137.52, 139.27, 149.386, 155.00, 155.67, 176.22 (C=O, carbonyl).

**2.3.2. Preparation of [Pb(ttpy)(μ-AcO)I]$_2$ (2).** Complex **2** was prepared in the same way as **1** using potassium iodide instead of ammonium hexafluorophosphate (0.3 g, yield 62%), m.p. 291°C. Anal. Calcd for $C_{24}H_{20}N_3O_2IPb$ (%): C, 27.13; H, 2.39; N, 6.00. Found (%): C, 27.45; H, 2.19; N, 6.06. IR (KBr) ($\nu_{max}$, $cm^{-1}$): 3020 (C–H, arom); 2855 (C–H, aliph); 1422–1603 (C=C, arom); 1398 [$\nu_{sym}$(COO)] and 1569 [$\nu_{as}$(COO)]; $^1$HNMR (DMSO) $\delta_H$: 1.68(3H, s, $CH_3$); 2.42(3H, s, $CH_3$); 7.41(2H, d, $^3J_{H-H} = 7.84$ Hz, arom); 7.61(2H, t, $^3J_{H-H} = 6.08$, 6.04 Hz, arom); 7.91(2H, d, $^3J_{H-H} = 7.76$ Hz, arom); 8.10(2H, t, $^3J_{H-H} = 7.75$, 7.69 Hz, arom); 8.70(2H, d, $^3J_{H-H} = 8.02$ Hz, arom); 8.75(2H, s, arom); 8.86(2H, d, $^3J_{H-H} = 4.36$ Hz, arom). $^{13}$CNMR (DMSO) $\delta_C$: 27.10, 117.63, 121.12, 125.01, 126.08, 130.06, 134.43, 137.51, 139.20, 149.32, 155.01, 155.71, 176.24 (C=O, carbonyl).

## 3. Results and discussion

### 3.1. *Spectroscopy*

Reaction of lead(II) acetate with 4′-p-tolyl-2,2′; 6′,2″-terpyridine (ttpy) in the presence of ammonium hexafluorophosphate or potassium iodide in methanol yielded crystalline materials of **1** and **2**, respectively. IR spectra of both complexes show absorptions resulting from skeletal vibrations of aromatic rings at 1421–1603 $cm^{-1}$ [27]. The relatively weak absorptions at 3038–3056 $cm^{-1}$ and 2855 $cm^{-1}$ are due to C–H modes of aromatic rings and aliphatics, respectively. Bands in the region 1395–1398 $cm^{-1}$ and 1569–1571 $cm^{-1}$ are assigned to $\nu_s$ and $\nu_{as}$ of acetate, respectively. In **1**, $\nu(PF_6)$ is a strong band at 839 $cm^{-1}$. The $^1$H NMR spectra of DMSO solutions of **1** and **2** display seven resonances assigned to CH protons of ttpy. Singlet resonances at 1.68–2.42 ppm are assigned to the methyl of acetate [27]. The $^{13}$C NMR spectra of the DMSO solution of both the complexes display 13 distinct resonances assigned to the aromatic and aliphatic carbons of ttpy.

### 3.2. *Crystal structures of complexes*

Complexes **1** and **2** crystallize in the triclinic system with space group $P\bar{1}$. Selected bond distances and angles are listed in table 2.

Table 2. Selected bond lengths (Å) and angles (°) for **1** and **2**.

| **1** | | **2** | |
|---|---|---|---|
| N1–Pb1 | 2.506(2) | Pb1–O1 | 2.353(5) |
| N2–Pb1 | 2.532(2) | Pb1–O2 | 2.890(6) |
| N5–Pb1 | 2.612(2) | Pb1–N1 | 2.558(7) |
| O2–Pb1 | 2.297(2) | Pb1–N2 | 2.491(6) |
| O1–Pb1 | 2.813(3) | Pb1–N3 | 2.515(5) |
| Pb1–Pb2 | 4.741(2) | Pb1–I1 | 3.424(1) |
| O1–Pb2 | 2.957(3) | Pb2–O1 | 2.948(1) |
| N1–Pb1–N2 | 65.55(7) | N2–Pb–N1 | 64.5(2) |
| N1–Pb1–N5 | 64.43(7) | N2–Pb–N3 | 65.3(2) |
| N1–Pb1–O2 | 84.83(7) | N1–Pb–N3 | 128.1(2) |
| N1–Pb1–O1 | 124.14(7) | O1–Pb–O2 | 48.1(2) |
| N2–Pb1–N5 | 127.64(7) | I1–Pb–N1 | 87.9(1) |
| N2–Pb1–O2 | 78.3(7) | I1–Pb–N2 | 74.1(1) |
| N2–Pb1–O1 | 121.69(7) | I1–Pb–N3 | 90.6(1) |
| N5–Pb1–O2 | 82.84(7) | I1–Pb–O1 | 157.0(1) |
| N5–Pb1–O1 | 76.91(7) | I1–Pb–O2 | 149.3(1) |



In both **1** and **2**, the crystal structures consist of dimeric units of [Pb(ttpy)(μ-AcO)]($PF_6$) and [Pb(ttpy)(μ-AcO)I], respectively (figure 1). Each lead is chelated by three ttpy nitrogen atoms and three acetate oxygen atoms (table 2). One acetate bridges between two lead ions to produce dimeric units in the solid state. The coordination number in **1** is six. Owing to the presence of iodide, the coordination number in **2** is seven.

The Pb–O distance for the μ-AcO bridge is rather long (2.957(3) in **1**, 2.948(3) Å in **2**), thus pointing toward the presence of sterically active electron lone pair on lead. The observation is supported by shortening of the Pb–O and Pb–N bonds on the side of the Pb(II) opposite to the putative lone pair of electrons (in **1**: Pb–O 2.506(2) Å, Pb–N 2.297(2) Å; in **2**: Pb–O 2.353(2) Å, Pb–N 2.491(2) Å). The N2–Pb–N5 angle in **1** is 127.647° and N1–Pb–N3 angle in **2** is 128.1°, which is related to the gap that is possibly occupied by a stereo-active lone pair of electrons on Pb(II) [28].

For **1**, the dihedral angle between C11–N2–C12 and C16–N5–C17 least-square planes is 20.88° while in **2** the dihedral angle between C5–N3–C1 and C11–N1–C15 least-square planes is 13.54°. The aromatic rings of the ttpy ligand are not coplanar. The observations may be due to steric effects caused by intramolecular and intermolecular hydrogen bonds among the ttpy ligand and hexafluorophosphates or iodides (figure 2). Inter and intra molecular hydrogen bonding and $\pi$–$\pi$ stacking interactions as well as the stereo-chemically active lone pair of electrons on Pb(II) in **1** and **2** are likely responsible for the crystal packing arrangements. P–F···H, C–O···H, and P–F···C interactions are present in **1** [29, 30] (table 3, figure 3). The P–F···H distance ranges from 2.452 to 2.666 Å (table 3), which indicates moderate to strong hydrogen bonds. In **2**, there are C–H···O and C–H···I interactions (table 3, figure 3). The C–H···O distance ranges from 2.473 to 2.566 Å, with weak hydrogen-bonding interactions being important for interactions of molecular complexes in the crystalline state [31]. All ttpy molecules lie parallel, forming a layer packing structure with an intermolecular distance of 3.309 Å for **1** and 3.506 Å for **2**, with typical $\pi$–$\pi$ stacking interactions in an offset fashion (slipped face-to-face with a distance of 3.999 Å in **1** and 3.943 in **2** (figure 4)).

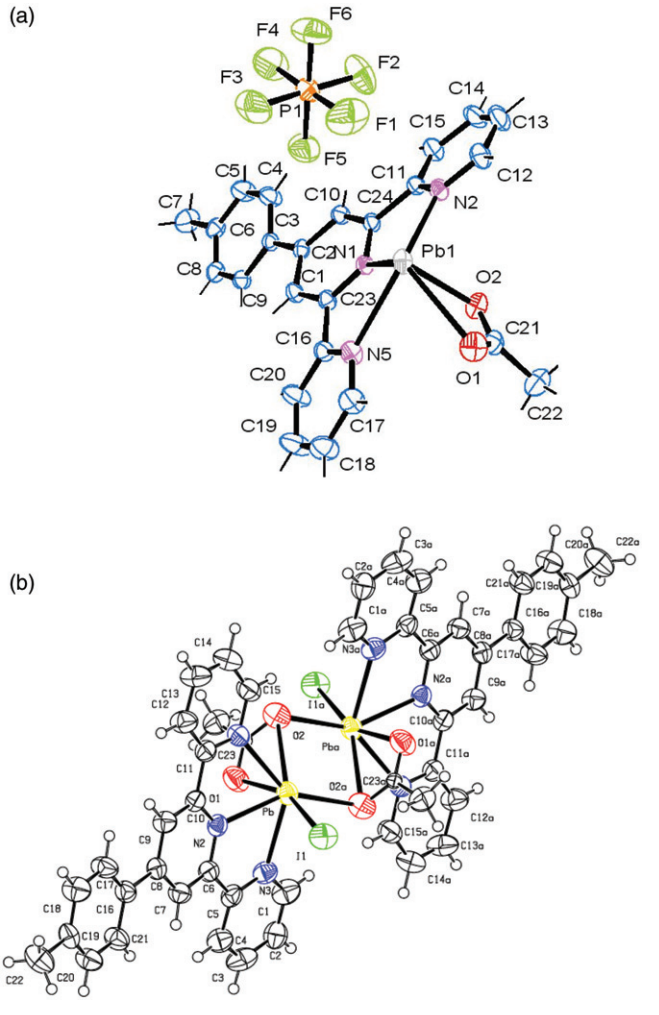


Figure 1. Ortep diagram of (a) $[Pb(ttpy)(\mu\text{-}AcO)]_2(PF_6)_2$ (**1**) and (b) $[Pb(ttpy)(\mu\text{-}AcO)I]_2$ (**2**).

The lone pair activity depends on (1) hard or soft bonding, (2) attractive or repulsive interactions among ligands, (3) the *p* character of lone pairs, and (4) the number of electrons (charge) transferred from the ligands to the metal [19]. Hence, the geometry of the nearest coordination environment of each lead is likely caused by interplay of several factors. The geometrical constraints of the coordinated ttpy, the counter ion, and influences of stereo-chemically active lone pairs of electrons result in a significant gap *trans* to ttpy and hemidirected coordination around lead is suggested [32].

Changing the anion from $PF_6^-$ to $I^-$ results in different crystal structures and packings. In other words, the two anions have different coordination behavior in forming lead complexes with ttpy. Because of poor coordination ability of $PF_6^-$, in comparison with $I^-$, coordination environment of complex changes from 6 to 7 in **1** and **2**, respectively. Thus, the anion has an important role in preparing these complexes and its coordinating nature causes changes in the crystal structure and packing system.

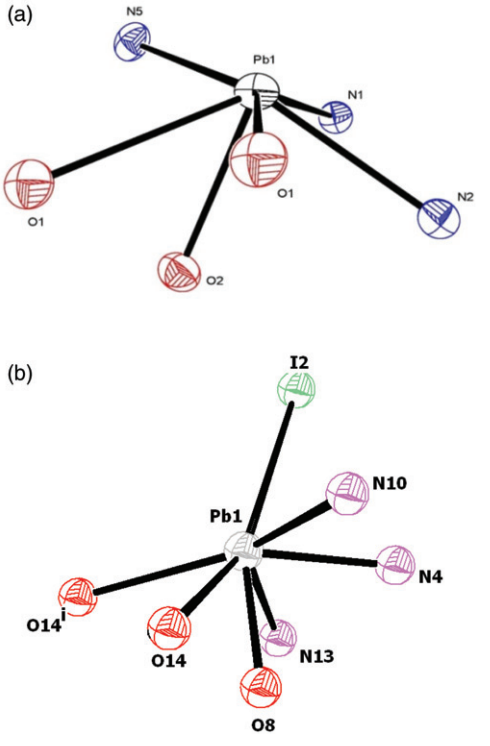


Figure 2. Schematic representation of (a) the six-coordinate Pb1 environment in **1** and (b) the seven-coordinate Pb1 center in **2**. There is a hole in the sphere of both Pb.

Table 3. Intermolecular distances for **1** and **2** (Å).

| **1** | | **2** | |
|---|---|---|---|
| O1···H12 | 2.621 | O1···H22 | 2.473 |
| O2···H7A | 2.559 | I1···H21 | 3.133 |
| F1···H22A | 2.657 | O2···H1 | 2.566 |
| F2···H13 | 2.653 | Pb···C23 | 3.462 |
| F3···H9 | 2.546 | H3···H3 | 2.341 |
| F4···H5 | 2.452 | H20···H24A | 2.042 |
| F5···C24 | 2.033 | C23···H24B | 2.821 |
| F6···H15 | 2.666 | H13···H24C | 2.250 |
| $\pi$–$\pi$ (slipped face to face) | 3.990 | $\pi$–$\pi$ (slipped face to face) | 3.943 |
| | | $\pi$–$\pi$ (slipped face to face) | 3.859 |
| $\pi$–$\pi$ offset | 3.309 | $\pi$–$\pi$ offset | 3.506 |

### 3.3. *Thermal gravimetric analysis*

To examine the thermal stability of **1** and **2**, thermal gravimetric analyses (TGA) were carried out between 30°C and 700°C (figure 5). These compounds are stable to 285°C and 296°C, respectively, at which temperature they begin to decompose. The TG curve

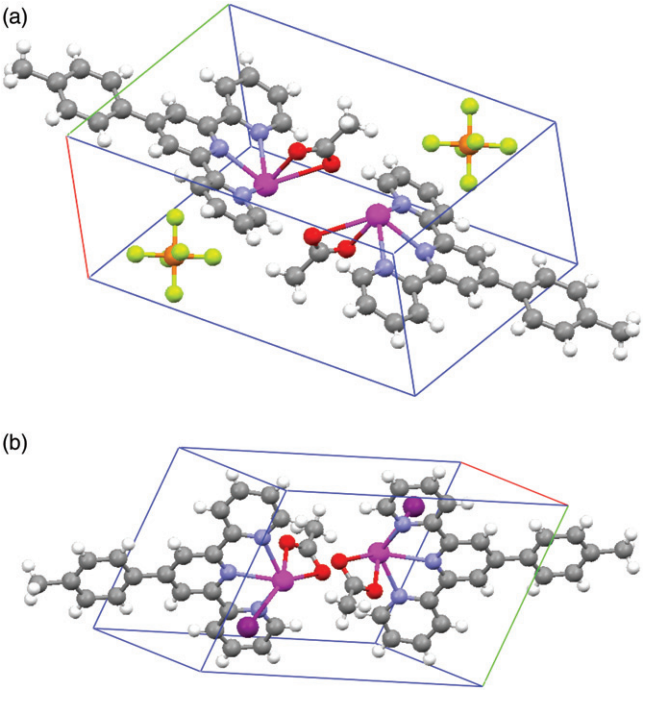


Figure 3. Unit cell of (a) **1** and (b) **2**.

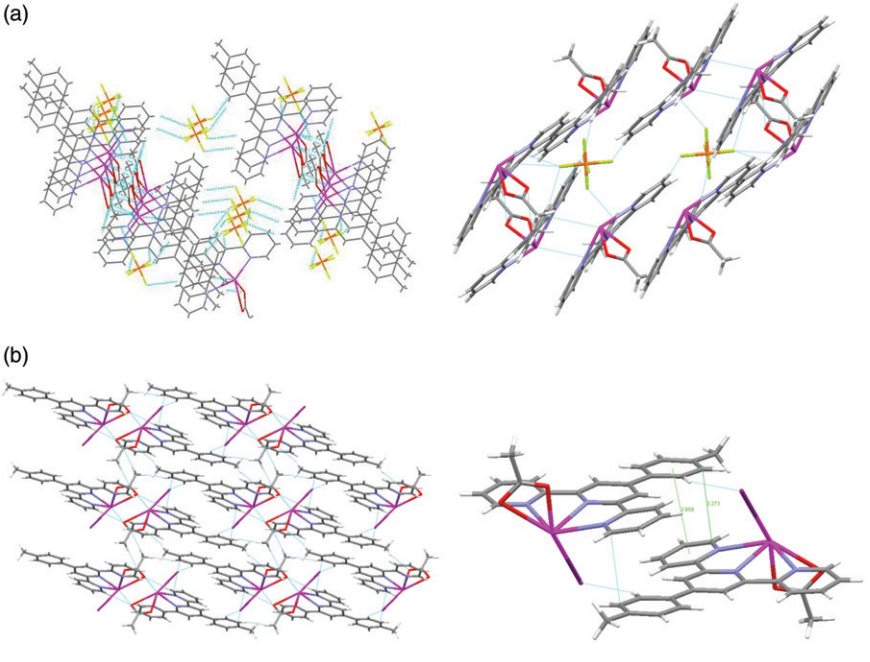


Figure 4. Packing diagram of (a) **1** and (b) **2** with intermolecular interactions shown as dotted lines.

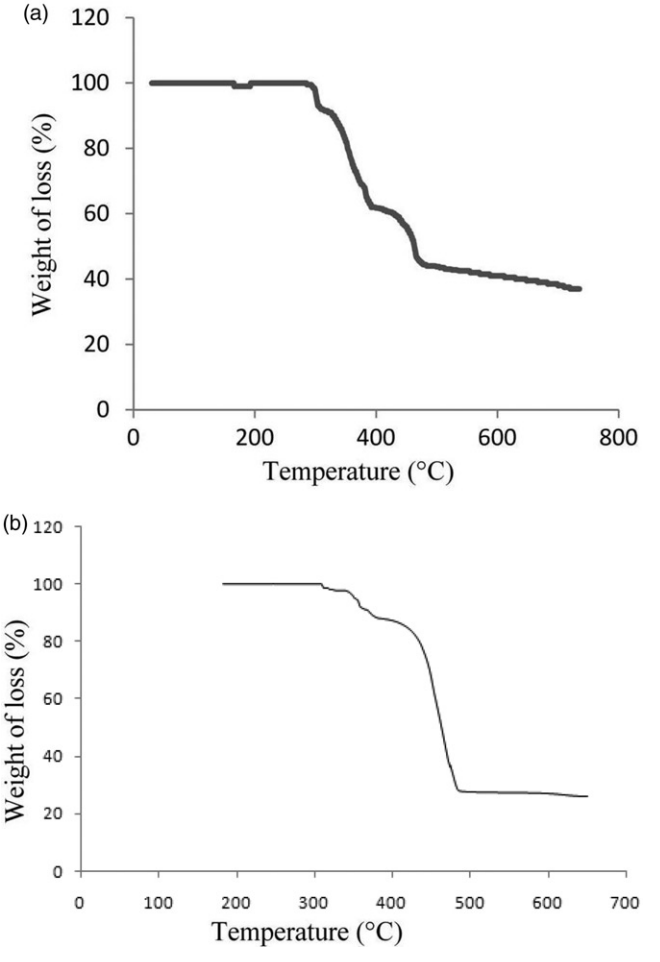


Figure 5. Thermal behavior of (a) **1** and (b) **2**.

of **1** indicates two exothermic transformations at 285°C and 316°C, which are related to the release of ttpy. The solid residue at 318°C is stable to 423°C and undergoes another exothermic transformation. Remaining solid residue undergoes very slightly exothermic transformation at 465°C, attributed to PbO (37%). The TG curve of **2** indicates three exothermic transformations at 296°C, 345°C, and 372°C, which are related to the release of acetate, iodide, and ttpy, respectively. The solid residue at 372°C is stable to 420°C and undergoes another exothermic transformation. The left out solid residue is suggested to be PbO (30%).

### 3.4. *Electrochemical studies of ttpy, 1 and 2*

The influence of scan rate on the electrochemical behavior of ttpy and $[Pb(ttpy)(\mu\text{-}AcO)]_2(PF_6)_2$ was investigated (figure 6a and b). The redox peak current

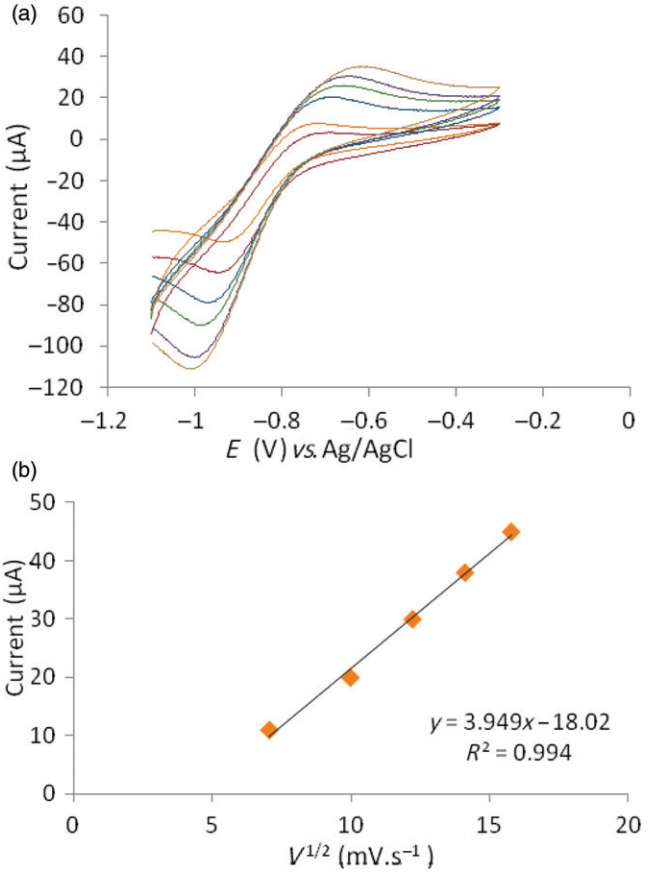


Figure 6. (a) Cyclic voltammograms of ttpy in various scan rates; (b) plot of square root of scan rate in ttpy.

of ttpy and Pb complex increases linearly with the increase of square root of scan rate, typical of diffusion-controlled process for ttpy and $[Pb(ttpy)(\mu\text{-}AcO)]_2(PF_6)_2$ (figure 7a and b). The cyclic voltammogram of ttpy exhibits a quasi-reversible oxidation peak at $-0.705$ V ($\Delta E_p = 182$ mV). The cyclic voltammogram of $[Pb(ttpy)(\mu\text{-}AcO)]_2(PF_6)_2$ exhibits irreversible oxidation at $+0.574$ V ($\Delta E_p = 439$ mV), which can be attributed to $Pb^{2+}/Pb^{4+}$ process. The influence of scan rate on the electrochemical behavior of ttpy and $[Pb(ttpy)(\mu\text{-}AcO)I]_2$ was investigated (figure 8a and b). The redox peak current of **2** increases linearly with the increase of square root of scan rate. The cyclic voltammogram of $[Pb(ttpy)(\mu\text{-}AcO)I]_2$ exhibits two irreversible oxidation peaks at $+0.599$ and $+0.831$ V ($\Delta E_p = 815$ mV), which can be attributed to the $Pb^{2+}/Pb^{4+}$ process. The anodic currents increase and the peak potential shifts toward positive direction (figure 8b) with increasing scan rate. When peak current values were plotted against $v^{1/2}$ (figure 8b), the following linear relationship was obtained:

$$I_p = 32.37 - 40.83v^{1/2}\,(mV^{1/2}s^{-1/2}); \quad R^2 = 0.986 \tag{1}$$

The behavior indicates that the oxidation of $Pb^{2+}/Pb^{4+}$ is controlled by diffusion. The charge transfer coefficient ($\alpha$) and the number of electrons involved in the

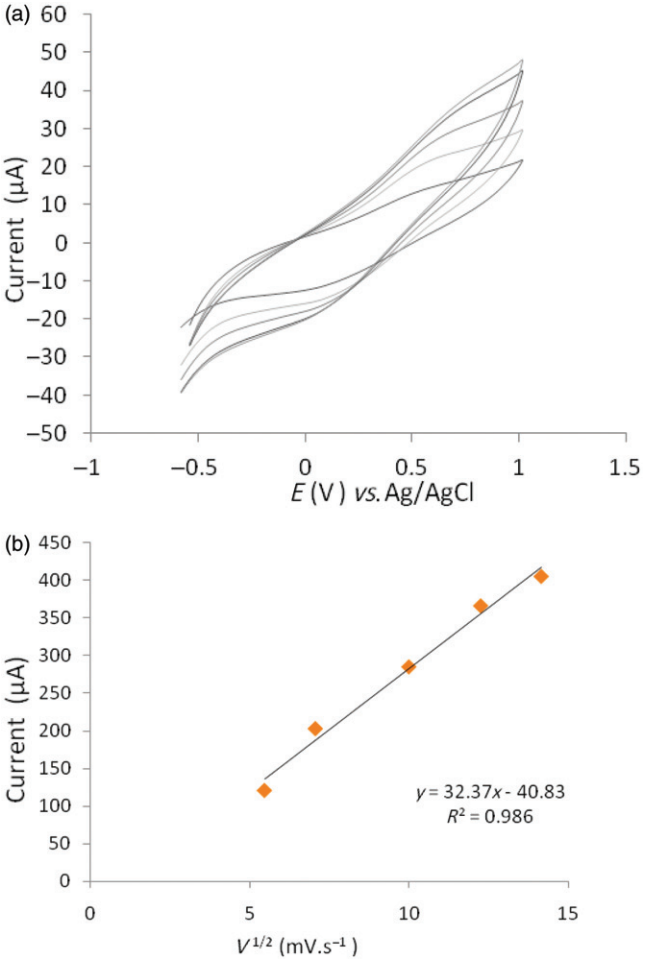


Figure 7. (a) Cyclic voltammograms of **1** in various scan rates; (b) plot of square root of scan rate in **1**.

rate-determining step ($n\alpha$) can be evaluated. The Tafel slope was 163 mV decade$^{-1}$. If $\alpha$ was assumed equal to 0.39, $n$ was equaled to $1.96 \sim 2$.

## 4. Conclusion

Syntheses, molecular, and crystal structures of two tridentate 4′-p-tolyl-2,2′; 6′,2″-terpyridine (ttpy) lead(II) complexes with 1 : 1 metal/ligand ratio, $[Pb(ttpy)(\mu\text{-}AcO)]_2(PF6)_2$ (**1**) or $[Pb(ttpy)(\mu\text{-}AcO)I]_2$ (**2**), with two types of counter anions are described in this article. Anionic effects on the formation of different crystallographic symmetry, molecular structures, and packing patterns for lead(II) complexes indicates that counter ions play important roles in the system. Electrochemical studies reveal that both lead(II) complexes show Pb(II) oxidation irreversibly *via* diffusion-controlled reactions.

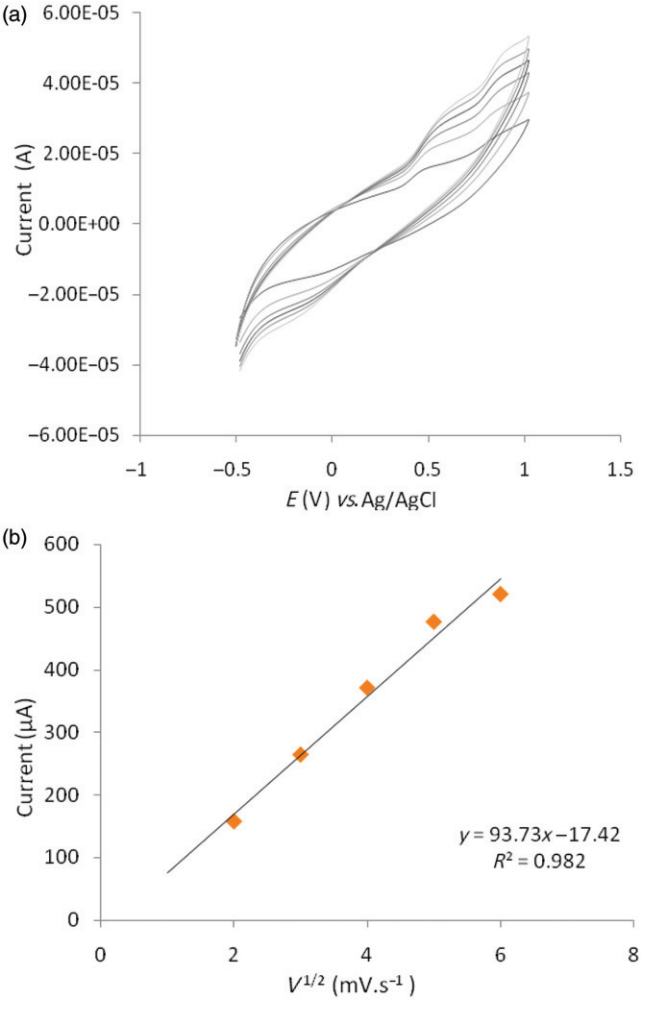


Figure 8. (a) Cyclic voltammograms of **2** in various scan rates; (b) plot of square root of scan rate in **2**.

## Supplementary material

CCDC reference numbers 842111 and 840137 contain the supplementary crystallographic data for this article. These data can be obtained free of charge at www.ccdc.cam.ac.uk/conts/retrieving.html

## Acknowledgments

Support of this investigation by the Payame Noor University, Islamic Republic of Iran, Universite du Maine, Le Mans, France, and Atatürk University, Erzurum, Turkey, is gratefully acknowledged.

## References


[1] D.J. Bray, J.K. Clegg, K.A. Jolliffe, L.F. Lindoy, G. Wei. *J. Coord. Chem.*, **61**, 3 (2008).
[2] N. Noshiranzadeh, A. Ramazani, A. Morsali, A.D. Hunter, M. Zeller. *Inorg. Chem. Commun.*, **10**, 738 (2007).
[3] L.F. Lindoy, I.M. Atkinson. *Self-assembly in Supramolecular Chemistry*, Royal Society for Chemistry, Cambridge, UK (2000).
[4] C. Kaes, A. Katz, M.W. Hosseini. *Chem. Rev.*, **100**, 3553 (2000).
[5] G.V. Oshovsky, D.N. Reinhoudt, W. Verboom. *Angew. Chem. Int. Ed.*, **46**, 2366 (2007).
[6] H. Hofmeier, U.S. Schubert. *Chem. Soc. Rev.*, **33**, 373 (2004).
[7] E.C. Constable. *Chem. Soc. Rev.*, **36**, 242 (2007).
[8] J.E. Beves, P. Chwalisz, E.C. Constable, C.E. Housecroft, M. Neuburger, S. Schaffner, J.A. Zampese. *Inorg. Chem. Commun.*, **11**, 1009 (2008).
[9] W. Spahni, G. Calzaferri. *Helv. Chim. Acta*, **67**, 450 (1984).
[10] C. Chamchoumis, P.G. Potvin. *J. Chem. Res., Synop.*, **4**, 180 (1998).
[11] J. Wang, G.S. Hanan. *Synlett*, **8**, 1251 (2005).
[12] J.S. Casas, M.S. Garcia-Tasende, J. Sordo. *Coord. Chem. Rev.*, **209**, 197 (2000).
[13] P. Bera, C.H. Kim, S.I. Seok. *Inorg. Chim. Acta*, **362**, 2603 (2009).
[14] A.R. Mahjoub, A. Morsali. *Polyhedron*, **21**, 1223 (2002).
[15] J. Parr. *Polyhedron*, **16**, 551 (1997).
[16] L.M. Engelhard, D.L. Kepert, J.M. Patrick, A.H. White. *Aust. J. Chem.*, **42**, 329 (1998).
[17] A.K. Hall, J.M. Engelhard, A. Morsali, A.A. Soudi, A. Yanovsky. *CrystEngComm*, **2**, 82 (2000).
[18] R.D. Hancock. In *Perspectives in Coordination Chemistry*, A.F. Williams, C. Floriani, A.E. Merbach (Eds), p. 129, VCHA, VCH, Basel (1992).
[19] R.D. Hancock, M.S. Shaikjee, S.M. Dobson, J.C.A. Boeyens. *Inorg. Chim. Acta*, **154**, 229 (1988).
[20] P. Pyykko. *Chem. Rev.*, **88**, 563 (1988).
[21] A. Bashall, M. Mcpartlin, B.P. Murphy, D.E. Fenton, S.J. Kitchen, P.A. Tasker. *J. Chem. Soc., Dalton Trans.*, 505 (1990).
[22] P. Schwerdtheger, G.A. Heath, M. Dolg, M.A. Bennett. *J. Am. Chem. Soc.*, **114**, 7518 (1992).
[23] K. Byriel, K.R. Dunster, L.R. Gahan, C.H.L. Kennard, J.L. Latten, I.L. Swann, P.A. Duckworth. *Polyhedron*, **11**, 1205 (1992).
[24] A. Morsali, A.R. Mahjoub. *Inorg. Chem. Commun.*, **7**, 915 (2004).
[25] N. Noshiranzadeh, A. Ramazani, A. Morsali, A.D. Hunter, M. Zeller. *Inorg. Chim. Acta*, **360**, 3603 (2007).
[26] (a) L.J. Farrugia. *J. Appl. Crystallogr.*, **30**, 565 (1997); (b) L.J. Farrugia. *CrystalClearTM Software*, Rigaku Inc., Texas, USA (2005); (c) G.M. Sheldrick. *SHELX-97 Program Package, SHELXS-97 and SHELXL-97*, University of Göttingen, Göttingen, Germany; (d) K. Brandenburg. *DIAMOND*, Crystal Impact GbR, Bonn, Germany (2001).
[27] (a) K. Nakamoto. *Infrared and Raman Spectra of Inorganic and Coordination Compounds Part B: Applications in Coordination, Organometallic, and Bioinorganic Chemistry*, 6th Edn, p. 121, John Wiley & Sons, Inc., Hoboken, New Jersey (2009);(b) K. Kam-Wing Lo, C.-K. Chung, D.C.-M. Ng, N. Zhub. *New J. Chem.*, **26**, 81 (2002); (c) L. Gou, Q.R. Wu, H.-M. Hu, T. Qin, G.-L. Xue, M.-L. Yang, Z.-X. Tang. *Polyhedron*, **27**, 1517 (2008); (d) D.H. Williams, I. Fleming. *Spectroscopic Methods in Organic Chemistry*, 4th Edn, McGraw Hill, London (1989).
[28] L. Shimoni-Livny, J.P. Glusker, C.W. Brock. *Inorg. Chem.*, **37**, 1853 (1998).
[29] (a) G.R. Desiraju, T. Steiner. *IUCr Monograph on Crystallography*, Vol. 9, Oxford Science, Oxford (1999); (b) J. Granifo, M. Vargas, M.T. Garland, A. Ibanez, R. Gavino, R. Baggio. *Inorg. Chem. Commun.*, **11**, 1388 (2008); (c) K.-L. Huang, C.-W. Hu. *Inorg. Chim. Acta*, **360**, 3590 (2007); (d) C. Janiak, T.G. Scharmann. *Polyhedron*, **22**, 1123 (2003).
[30] A.C. Moro, F.W. Watanabe, S.R. Ananias, A.E. Mauro, A.V.G. Netto, A.P.R. Lima, J.G. Ferreira, R.H.A. Santos. *Inorg. Chem. Commun.*, **9**, 493 (2006).
[31] J.W. Steed, J.L. Atwood. *Supramolecular Chemistry*, John Wiley & Sons, Ltd., Chichester, UK (2000).
[32] K. Biradha, K.V. Domasevitch, B. Moulton, C. Seward, M.J. Zaworotko. *Chem. Commun.*, 1327 (1999).